Excited State Proton Transfer in Indole-2-carboxylic Acid and Indole-5-carboxylic Acid

Prakriti Ranjan Bangal and Sankar Chakravorti*

Department of Spectroscopy, Indian Association for the Cultivation of Science, Jadavpur, Calcutta 700032, India

Received: June 9, 1999

Intramolecular excited state proton transfer in indole-2-carboxylic acid (I2C) and indole-5-carboxylic acid (I5C) was investigated in various solvents in acidic, basic, and neutral media by steady state and time-resolved fluorescence spectroscopy. Hidden dual fluorescence of I2C in polar and nonpolar solvents and distinct dual fluorescence of I5C in nonpolar solvents and broad structureless fluorescence band in polar solvent (which is composed of two fluorescence bands) are assigned to be arising out from Franck−Condon excited state and from proton transferred excited state, i.e., from zwitterionic form, respectively. The modulation of proton transfer equilibrium constant in β-CD cavity has also been investigated for both the molecules. For I5C it has been observed that in protic solvents intramolecular proton transfer is blocked by H-bond formation with solvent molecules surrounding it but when it enters into the β-CD cavity intramolecular proton transfer in the excited state could be observed again. The excited state proton transfer equilibrium constant was calculated from a fluorescence band shape analysis, and its large solvent dependence arises primarily from local solute−solvent interaction. As the instrument time resolution was 500 ps, only monoexponential fluorescence decay could be observed for all excitation wavelengths and this showed that the proton transfer (rise time) was considerably faster than fluorescence decay. Structural change and large dipole moment in the excited state as revealed from quantum chemical calculations with AM1 Hamiltonian point to the tendency of proton transfer in first excited singlet state and also hindrance of that in the ground state.

1. Introduction

Molecules of diverse nature and complexities have been the subject of investigations from different angles but possibly aromatic molecules containing acid and base moieties have attracted special attention for decades toward excited state proton transfer due to their paramount importance in chemistry and biochemistry.[1−3] Proton transfer presents the most fundamental processes involved in chemical reactions and in living systems.[4] Ground state proton transfer reactions are the simplest and most important processes found in chemistry. They have an outstanding place in general chemistry (chemical physics). More than 30 years ago Weller published his new classic paper[5] on excited state intramolecular proton transfer (ESIPT) in salicylic acid which triggered research on this subject in many laboratories.[6−12] Yet, excited state proton transfer (ESPT) is much less popular even in the realm of photochemistry despite their unquestionable importance in fundamental and applied photochemistry. When either the acidic or basic moieties of the same molecule became stronger acids or bases in excited states, proton transfer (PT) may occur rapidly in the excited state to form a tautomer. The majority of reactions of this type involve the transfer of a proton from an oxygen donor to an oxygen or nitrogen acceptor. Here, an important point to note is that few cases are known where a nitrogen atom can function as donor and a carbon atom as the acceptor. An intramolecular proton transfer is facilitated in the excited state if there is an intramolecular hydrogen bond between two moieties in ground state. The importance of this H bond is such that it is convenient to discuss its nature. Intramolecular proton transfer reactions have been applied in chemical lasers,[13] energy storage systems and information storage devices at a molecular level,[9] high-energy radiation detectors,[14] and polymer stabilizers.[15,16] Due to all such possible interesting outcomes, different groups throughout the world are working with a wide variety of fluorescing acid−base containing molecule in order to systematize and control their emissive properties.

In a preliminary note,[17] the dual fluorescence of indole-2-carboxylic acid and indole-5-carboxylic acid was reported. As indole is a considerably stronger proton acceptor, the compounds are distinguished by their difference in intramolecular hydrogen bond strength. Now, in this paper we will report a detailed investigation of the fluorescent properties of these compounds in different solvents and also in β-cyclodextrin with a view to understand different aspects of excited state intramolecular proton transfer. Quantum semiempirical calculations were performed to discern the nature and mechanism of proton transfer.

2. Experimental Section

The compounds indole-2-carboxylic acid (I2C) and indole-5-carboxylic acid (I5C) were purchased from Aldrich Chemical Co. and were purified by vacuum sublimation.

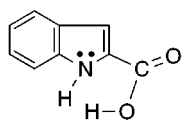

indole-2 carboxylic acid (I2C)

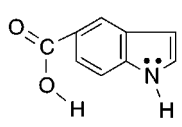

indole-5 carboxylic (I5C)

β-Cyclodextrin (β-CD) (Aldrich) was used as supplied. The solvents ethanol (EtOH), acetonitrile (ACN), tetrahydrofuran (THF), diethyl ether (DEE), chloroform ($CHCl_3$), dioxane,

* Corresponding author. E-mail: spsc@mahendra.iacs.res.in.

10.1021/jp991884f CCC: $18.00
Published on Web 10/14/1999

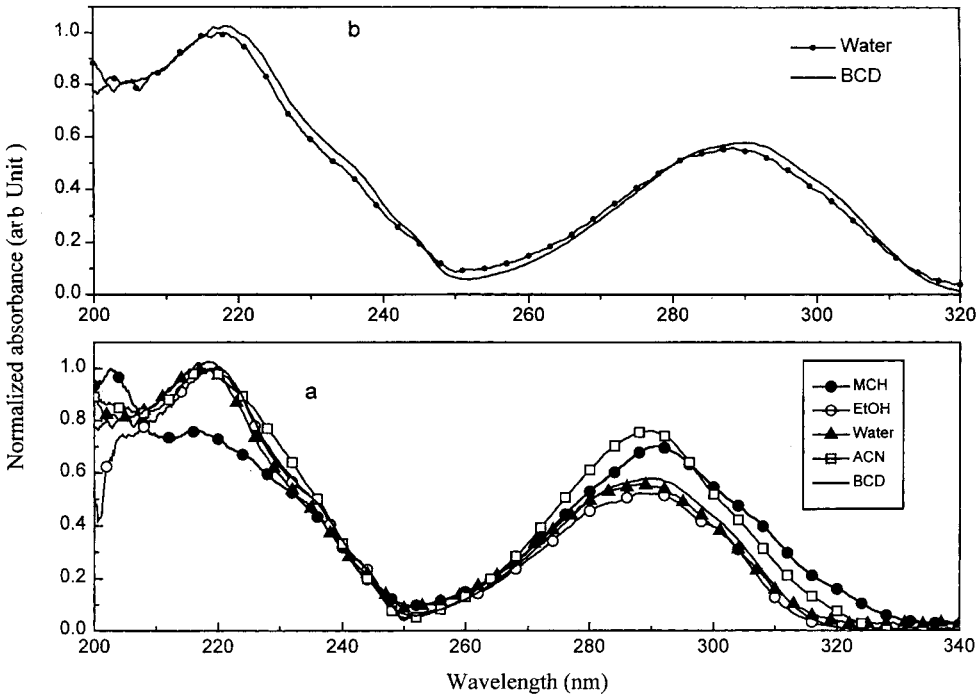

Figure 1. (a) Electronic absorption spectra of I2C in different solvents. (b) Electronic absorption spectra of I2C in water and β-CD.

sulfuric acid, and triethylamine (TEA) (E. Merck, spectroscopic grade) were used as supplied, but only after checking the purity fluorimetrically in the wavelength range of interest. Methylcyclohexane (MCH), *n*-hexane (CH), and carbon tetrachloride (CCl_4) (E. Merck spectroscopic grade) were used after distillation (dry) and checking of any emission in the required wavelength range. For aqueous solution, we used deionized MilliPore water.

The absorption spectra at 300 K were recorded with a Shimadzu absorption spectrophotometer model UV-2101PC, and the fluorescence spectra were obtained with a Hitachi F-4500 spectrofluorometer. For emission measurement, the sample concentration was maintained at 10^{-5} M in each case in order to avoid aggregation. The quantum yields were determined by using the secondary standard method with recrystallized indole in cyclohexane ($\varphi_f = 0.4$) described elsewhere.[40] The fluorescence lifetime measurement was performed by time-correlated single photon counting coupled to a microchannel plate photomultiplier (model 28090, Hamamatsu, Edinburgh Instrument).

3. Results and Discussion

3.1. Absorption Spectra. The absorption spectra of indole-2-carboxylic acid (I2C) and indole-5-carboxylic acid (I5C) show broad structureless bands in different organic polar, nonpolar aqueous solutions and in restricted geometry such as β-CD cavity. Figure 1 and Figure 2 show the absorption spectra of I2C and I5C in different environments, respectively. The absorption spectra of I2C show a peak in the region of 288−290 nm on solvent dependence (Table 1) whereas the absorption spectra of I5C exhibit flat and broad absorption bands having no trace of distinct peaks. We could expect a maximum absorbance in the region of 272−275 nm. The molar extinction coefficients of the first absorption maxima (lower energy band) of I2C and I5C in all solvents are very high (Table 1) showing a character of (π, π^*) transitions for the first absorption band. It is also important to note that in hydrocarbon solvent, I2C shows two shoulders in the absorption band at 310 and 320

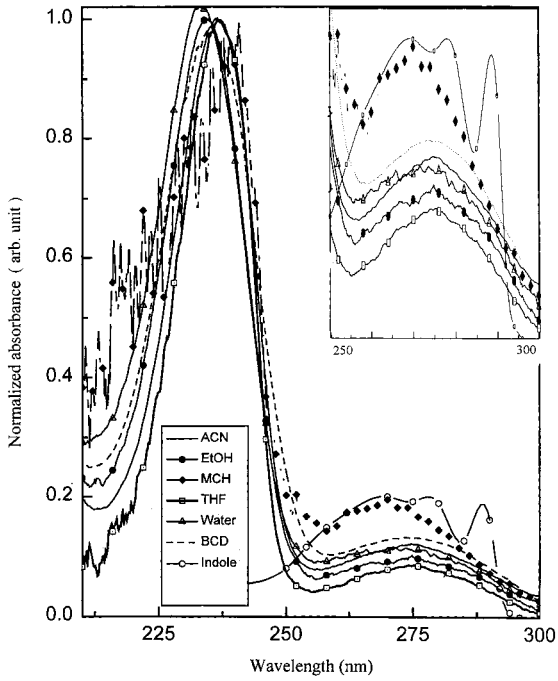

Figure 2. Electronic absorption spectra of I5C in different solvents and electronic absorption spectra of indole−MCH. Inset is the enlarged view of the lower energy portion of the spectra.

nm. In polar or hydroxylic solvent, these shoulders vanish, producing a more structureless broad band. If we compare this absorption spectrum of I2C with that of the parent compound indole, we find very little similarity between the two. This spectral change and appearance of lower energy shoulder in absorption spectra of I2C in hydrocarbon solvent results from 2-carboxylic acid substitution as well as from intramolecular hydrogen bonding between the acid and basic groups of the molecule. Also, it is important to note here that this red-shifted shoulder band in the hydrocarbon solvent and structureless tail account for the ground state closed tautomeric form. The disappearance of the lower energy shoulder in polar or hy-

TABLE 1: Absorption and Emission Data of I2C and I5C

	I2C					I5C				
	ϵ_{max}[a] at lower	abs	fluorescence peak			ϵ_{max}[a] at lower	abs	fluorescence peak		
solvent	energy band	maxima (nm)	λ_f^1 (nm)	λ_f^2 (nm)	total φ	energy band	maxima (nm)	λ_f^1 (nm)	λ_f^2 (nm)	total φ
MCH	3530	289	332	374	0.15	2910	273	337	405	0.2
MCH + TEA	3538	288	332		0.09	2920	273	337		0.1
MCH + H_2SO_4	3533	289		380	0.07	2921	274		413	0.08
n-hexane	3495	287	333	372	0.14	2929	275	337	402	0.21
THF	3399	286	334	381	0.16	2898	275	338	415	0.17
DEE	3553	286	334	377	0.11	3001	275	338	410	0.11
dioxane	3595	286	334	380	0.1	2998	275	338	414	0.13
$CHCl_3$	3499	287	334	379	0.12	2999	276	338	412	0.15
ACN	3691	285	335	384	0.2	2819	274	339	422	0.25
N,*N*-DMF	3609	285	335	384	0.21	2820	275	338	420	0.25
EtOH	3399	284	334	382	0.13	3019	275			0.08
water	3432	284	335	386	0.22	3030	274			0.05
β-CD + H_2O	3455	287	335	380	0.16	3039	273	340	421	0.12

[a] In $dm^3\ cm^{-1}\ mol^{-1}$.

TABLE 2: IR Data of I2C and I5C

samples	ν_{N-H} (cm^{-1})	$\Delta\nu_{N-H}$ (cm^{-1})	$\nu_{C=O}$ (cm^{-1})	ν_{O-H} (cm^{-1})	$\Delta\nu_{O-H}$ (cm^{-1})	E_{hb} (kcal mol^{-1})
I2C	3357	85	1667	3052	548	11.56
I5C	3360	88	1669	3150	450	9.8

droxylic solvents due to increase of solute−solvent interactions causes mainly loss of structure.

Again, if we consider the absorption spectra of I5C with respect to the absorption spectra of indole, we observe a vast change in spectral distribution. Irrespective of solvents properties, I5C shows flat bands (from 250 to 300 nm) with lower absorbance producing no sharp peaks. This change of absorption spectra is associated only with the redistribution of charge in excited state. So we can infer that the introduction of carboxylic group in the 5-position of the parent molecule is responsible for this redistribution of charge through the intramolecular hydrogen bond formation between the carboxylic group and the basic group of the molecule in ground state. Now the difference in spectral behavior of I2C and I5C could be understood by the distance of two intramolecular acid base moieties. In I2C this distance is very small compared to that of I5C. Due to the increase of this moiety's distance, the ground state tautomeric form could be forbidden in I5C. Thus tautomeric form of I2C is the reason for the difference between the absorption spectra of the two molecules.

Finally, we have studied the effect on absorption spectra in a constrained cavity, i.e., in aqueous β-CD solution. In the case of I2C, as the β-CD concentration is increased, the absorbance maxima are red-shifted, and the absorbance of the maxima are increased, accompanied by four distinct isosbestic points at 211, 247, 281, and 312 nm (Figure 1). This finding confirms that in water solution of β-CD a caged species of I2C with a 1:1 stoichiometry is formed. But in the case of I5C, absorbance gradually increases along with very little red shift of absorption maxima with gradual addition of β-CD in the solution. No isosbestic point could be observed in the longer wavelength absorption band but one isosbestic point is observed at 236 nm on the shorter wavelength band which rules out the only possibility of having a single equilibrium involving one to one complexation between the probe molecule and β-CD.[18] Cyclodextrin complexes differing from 1:1 stoichiometry have been reported by several groups.[18−21] Two possibilities are proposed for this deviation. First, more than one guest molecule can be accommodated within a single β-CD cavity. Second, due to the space restriction more than one type of complex, each having 1:1 stoichiometry, might be formed. The slight increase in absorbance is presumably due to the detergent effect of β-CD and is attributed to the additional dissolution of I2C and I5C absorbed on the surface of the walls of the container.[18,19]

3.2. Intramolecular Hydrogen Bond in the Ground State. In order to evaluate the strength of hydrogen bonds and orientation of carboxylic group in I2C and I5C, the IR spectra were taken in KBr pellets. Table 2 shows the characteristic IR frequencies (O−H, C═O, and N−H stretching) of I2C and I5C. The (O−H) stretching bands (ν_{OH}) are found to appear at considerable lower frequencies compared to carboxylic acid (1-naphthol),[22] and also significant decrease in N−H stretching frequencies (ν_{N-H}) of I2C and I5C can be seen relative to those of indole derivatives.[22,23] These drastic changes in IR spectra certainly point to the fact that for both molecules there is a strong intramolecular hydrogen bond in the ground state and which is preferentially between the hydrogen of the OH group and the nitrogen atom of parent indole ring. But no change in C═O stretching frequencies could be observed for both the compounds. This observation confirms that there is no hydrogen bonding between oxygen atom of carbonyl group and the hydrogen atom of N−H. Using the following Badger−Bauer relation[24,25] we can easily calculate, the hydrogen bond energy (E_{hb}).

$$\Delta\nu_{OH}/\nu_{OH} = -K_{OH}E_{hb} \quad (1)$$

where $\Delta\nu$ and K are the magnitude of the spectral shift and proportionality coefficient reported to be 1.7×10^{-2} mol $kcal^{-1}$.[26] According to the above relation one can estimate the strengths of intramolecular hydrogen bond of I2C and I5C in the ground state as 11.5 and 7.85 kcal mol^{-1}, respectively.

3.2. Fluorescence Spectra. Indole is a highly fluorescing agent, but its one derivatives oxindole, in which one hydrogen atom is replaced by a oxygen atom in the 2-position of indole makes it a nonfluorescing molecule.[27] Here we report on the fluorescence properties of another two indole derivatives where in the 2- and 5-positions a carboxylic acid group has been substituted in place of hydrogen atom.

Indole-2-carboxylic acid (I2C) shows moderately high fluorescence at room temperature, having a bathochromic shift of fluorescence maxima with increasing solvent polarity. Figure 3 shows the fluorescence spectra of I2C in different solvents. In nonpolar hydrocarbon solvent the fluorescence spectra of I2C

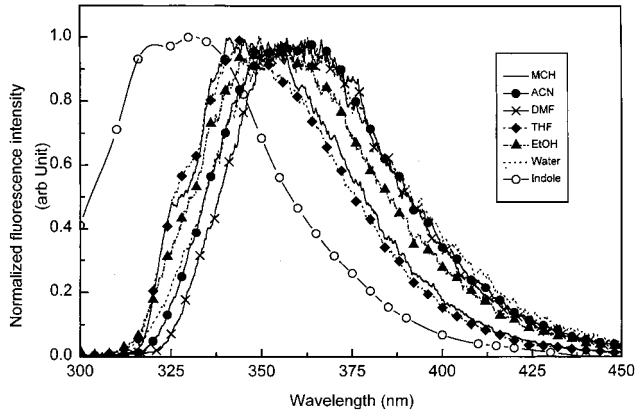

Figure 3. Fluorescence emission spectra of I2C in different solvents, and fluorescence emission spectra of indole in MCH at room temperature.

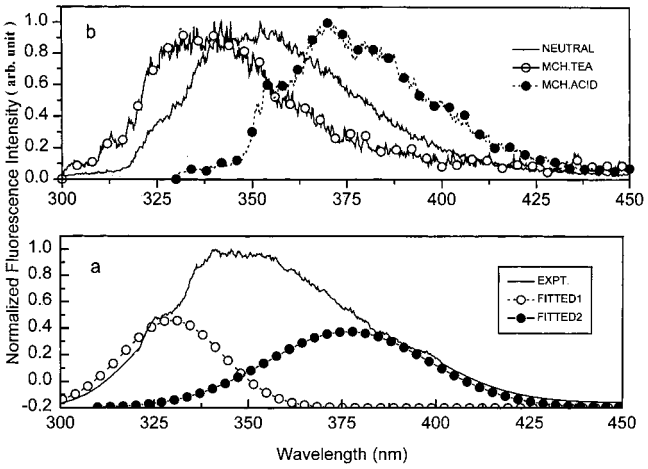

Figure 4. (a) Band-shape analysis of fluorescence spectra I2C in MCH. (b) Fluorescence spectra of I2C in neutral, acidic, and basic MCH.

shows two distinct bands peaking at around 330 and 370 nm. But in polar solvent like ACN one could observe a strong band at 384 nm. In hydroxylic medium, i.e., in ethanol, or in aqueous solution, I2C shows the same stucturelessbroad fluorescence spectra like that in ACN solution. In polar protic and aprotic solution, the higher energy band intensity reduces, making a broad band in the 370−386 nm wavelength region (Table 2). In comparison to the fluorescence spectra of indole, the appearance two band fluorescence spectra of I2C in MCH solution, indicates excited-state proton transfer in hydrocarbon solution. The first higher energy band (332 nm) is the normal fluorescence of indole (Figure 3), and the second lower energy band is the proton transfer band. Replacing hydrocarbon by more polar solvent (ACN, DMF), the higher energy band intensity reduces and the lower energy band intensity increases, resulting in a red-shifted broad structureless emission spectra. The half-width of the fluorescence spectra in all solvents is higher than that of the indole fluorescence spectra. This change in fluorescence spectra has been attributed to the fluorescence of the zwitterionic form resulting from excited state proton transfer. To confirm analytically, the fluorescence spectra of I2C in polar and nonpolar acidic and basic solution have been observed. In presence of triethylamine (TEA) in methylcyclohexane and acetonitrile solvent, I2C shows very weak (Table 2) fluorescence peaking at 332 nm but in the presence of H_2SO_4 it shows broad structureless fluorescence band at the longer wavelength region (Figures 4 and 5) both in nonpolar and polar medium. This spectral behavior in acidic and basic solution indicates that the

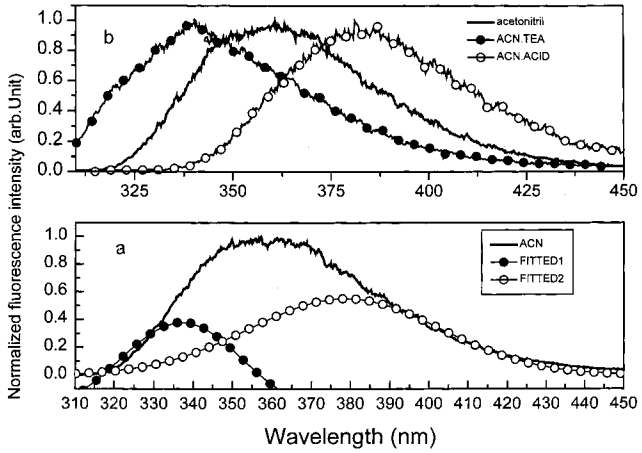

Figure 5. (a) Band-shape analysis of fluorescence spectra I2C in ACN. (b) Fluorescence spectra of I2C in neutral, acidic, and basic ACN.

SCHEME 1

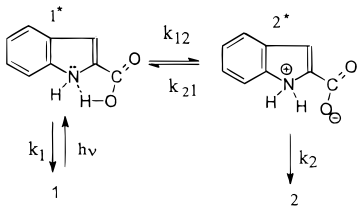

332 nm higher energy band and 380 nm lower energy fluorescence band are due to anionic and protonated form of I2C, respectively. A band-shape analysis was performed to the fluorescence spectra of neutral polar and nonpolar solution of I2C in order to obtain the shapes of two bands under the large envelope and at the same time to obtain the qualitative idea for equilibrium between the zwitterionic form and the normal form. Comparing fluorescence spectra of I2C with the fluorescence spectra of indole, we assign the two bands are arising out from **1*** and **2*** accordingly to Scheme 1. For this purpose the higher energy band measured for I2C in MCH was assumed as the fluorescence of pure neutral form **1***. This spectrum was fitted to the higher energy flank of the measured spectrum in polar solvent and in this procedure a small solvent shift was allowed. Figures 4 and 5 show the analyzed band position in MCH and ACN solution, respectively. Surprisingly, it is found that in all cases (i.e., for higher energy and lower energy band) the fitted bands lie in positions exactly identical with the bands obtained in acidic, basic ACN, and MCH solution separately. The maximum red shift is considerable enough as a consequence of larger stabilization of the zwitterionic form in excited state compared to the vertical ground state.

Normally, the organic hydroxylic solvent (ethanol) and water have a large tendency to form intermolecular hydrogen bonding with each other and solute present within it.[28] But in the case of I2C no trace in fluorescence spectra has been identified to detect the hydrogen bond formation with solvent molecules. So we can conclude that in the hydroxylic medium, excited state intramolecular proton transfer occurs similar to other polar solvents supporting Scheme 1. In this respect we observed the modulation of the fluorescence spectra of I2C in aqueous β-CD solution. For maximum concentration of β-CD in aqueous solution, the fluorescence maximum of the β-CD and I2C complex is slightly blue-shifted. On decreasing the β-CD concentration in solution, the fluorescence spectra are shifted toward red and finally they overlap the fluorescence spectra of I2C in aqueous solution. This blue shift of fluorescence spectra

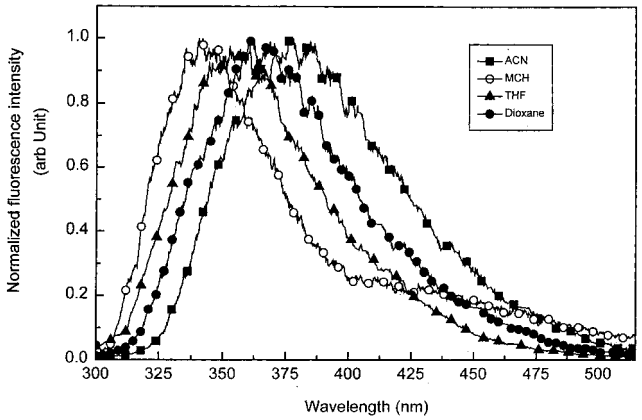

Figure 6. Fluorescence emission spectra of I5C in different solvents at room temperature.

is produced due to the lower polarity of the β-CD cavity.[29] When the probe molecule enters into the cavity, it faces a less polar environment, which is reflected by lower stabilization of the zwitterionic form and results in the small blue shift in the fluorescence spectra.

Figure 6 shows the fluorescence spectra of I5C in different solvents at 300 K. The fluorescence spectra of I5C show strong solvent-dependent properties. In hydrocarbon medium, I5C exhibits distinct dual fluorescence with higher energy band at 337 nm and lower energy band at 400 nm on excitation by wide range of absorption band keeping the fluorescence intensity and quantum yield as well as band shape unaltered. The excitation spectra corresponding to the two peaks are identical to each other and closely resemble the absorption spectrum. This shows that the two fluorescence bands originate from the same excited state. In comparison to indole (Figure 3) the higher energy fluorescence band of I5C is assigned to the neutral fluorescence of indole group and the lower energy band is due to excited state proton transfer. On placing the I5C in a polar aprotic solvent, the lower energy emission increases and the higher energy emission decreases, producing a large broadened envelope of total fluorescence. This indicates that the rate of excited state proton transfer reaction increases in polar solvents. With addition of a small amount of TEA in nonpolar and aprotic polar solution of I5C, the fluorescence spectrum turns into a fluorescence spectrum of indole having a peak at 337 nm wavelength with very low quantum yield (Table 2). This spectrum confirms that it is due to anionic form of I5C. On the other hand, addition of H_2SO_4 in both nonpolar and aprotic polar solutions of I5C changes the fluorescence spectra a lot. Only the lower energy fluorescence band appears with comparatively lower quantum yield. This result confirms that the appearance of the long-wavelength sideband is due to the protonated form of I5C. From band-shape analysis, we find two distinct peaks, under the envelope of broad structureless emission spectra. In this case also, the higher energy band obtained by addition of amine and the lower energy band obtained by addition of acid beautifully coincide with the two bands obtained from band-shape analysis (Figure 7). We consider here the two bands arising out from neutral and proton transfer conformer, respectively (Scheme 2). The fluorescence emission spectra of I5C in different hydroxylic solvents, including water, show the same large Stokes-shifted band with comparatively lower quantum yield than other nonhydroxylic solvents. The addition of a small amount of amine (triethylamine TEA) reduces the fluorescence intensity as well as quantum yield, keeping the band shape unaltered.

Figure 8 shows the fluorescence emission spectra of I5C as a function β-CD concentration. On increasing the β-CD

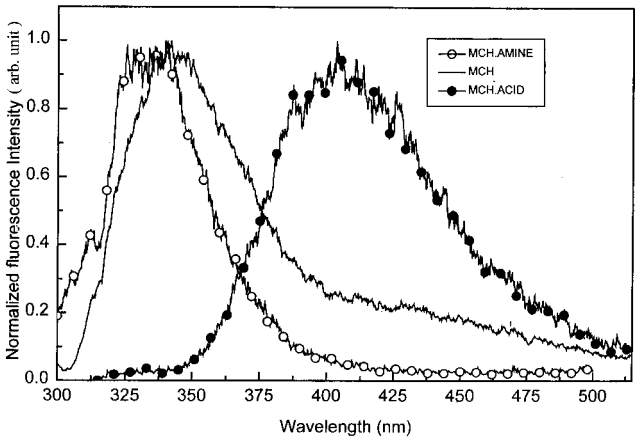

Figure 7. Fluorescence spectra of I5C in neutral, acidic, and basic MCH.

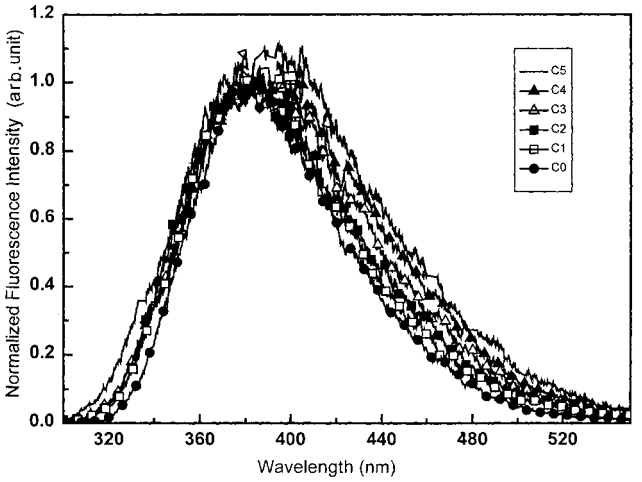

Figure 8. Fluorescence spectra of I5C as a function of β-CD concentration. The concentration of β-CD: $C_0 = 0$, $C_1 = 0.75$ mM, $C_2 = 1.5$ mM, $C_3 = 3$ mM, $C_4 = 6$ mM, $C_5 = 12$ mM.

SCHEME 2

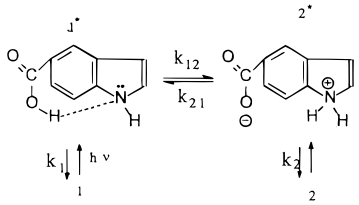

concentration, the fluorescence intensity as well as quantum yield increases, having the signature of a large bathochromic shift of the fluorescence maxima. As a result of this, one can observe total red-shifted intense fluorescence spectra compared to the that in aqueous solution. The half-width of the total fluorescence band is more in β-CD solution than that of the fluorescence in aqueous solution. This increase in half-width of fluorescence spectra in β-CD solution tempted us to perform band-shape analysis. Band-shape analysis confirms that the appeared fluorescence spectrum in β-CD solution is the composition of two hidden bands at 335 and 418 nm respectively. Ethanol and water as solvent have strong hydrogen-bonding strength.[28] In I5C, the acid and base moiety distance is higher than that of I2C, and the intramoleculer hydrogen bonding is rather weak in I5C. Due to this weak intramolecular hydrogen bonding between acid−base moieties, the presence of hydroxylic solvent disrupts this bonding and solute−solvent interaction is achieved through intermolecular hydrogen bond-

ing. So, in hydroxylic solvent the fluorescence species is mainly anionic in nature. Decrease in fluorescence intensity in the presence of amine confirms the intermolecular hydrogen bonding between water/ethanol and I5C. But when the molecule is encapsulated by the β-CD cavity, we observe only intramolecular phenomenon. In this case, the dual fluorescence is supposed to obtain from excited state proton transfer and the neutral conformer.

Now, considering the excited state equilibrium between the neutral and doubly ionized form (zwitterionic form) according to Schemes 1 and 2 (for both the molecules), the excited state equilibrium constant K' can be defined by the ratio of concentration of the **1*** and **2*** excited states:

$$K' = [\mathbf{2}^*]/[\mathbf{1}^*] \tag{2}$$

For steady state

$$K' = k_{12}/(k_2 + k_{21}) \tag{3}$$

where k_1 (k_2) are the decay rates of **1*** (**2***) and k_{12} (k_{21}) are the proton transfer **1*** $\rightarrow$ **2*** (**2*** $\rightarrow$ **1***) interconversion rate constant, respectively. If the back reaction is considerably faster than the decay of **2*** ($k_{21} \gg k_2$) then K' becomes equal to the ratio of the interconversion rate.

In I2C, the acid−base groups are very close to each other compared to I5C. Hence we expect a faster back reaction (2* $\rightarrow$ 1*) in I2C, resulting in the lowering of the second fluorescence band intensity. From our experiment we observed the same, i.e., the second band intensity is higher in I5C than that of I2C. So in I2C, K' becomes equal to the interconversion rates K' (k_{12}/k_{21}).

The ratio of quantum yields for the two bands and are then related to K' by

$$\frac{q_f^2}{q_f^1} = \left(\frac{k_{F2}}{k_{F1}}\right)K' \tag{4}$$

where k_{F1} and k_{F2} represent the inverse of the natural lifetimes of both structures, i.e., normal zwitterionic form and q_f^1 and q_f^2 are the fluorescence quantum yield of **1*** and **2*** in Schemes 1 and 2, respectively. Assuming k_{F1} and k_{F2} to be independent of solvent, the ratio of quantum yields is proportional to K'. k_{F1} for I2C and I5C are determined from quantum yield and measured lifetime data in MCH (since in MCH norrmal fluorescence is prominent) and for the molecules are determined similarly from quantum yield and lifetime data in ACN (since in ACN proton transfer fluorescence is prominent). $\tau_F = \tau_f^0 \varphi_f$ where is measured lifetime, is natural lifetime or intrinsic lifetime and is quantum yield.

$$k_F = \frac{1}{\tau_f^0} = \frac{\varphi_f}{\tau_f} \tag{5}$$

Now intrinsic decay rates for I2C are

$$k_{F1} = \frac{0.15}{2.21 \times 10^{-9}} = 6.787 \times 10^7\ s^{-1}$$

$$k_{F2} = \frac{0.2}{4.048 \times 10^{-9}} = 4.94 \times 10^7\ s^{-1}$$

Similarly, intrinsic decay rates k_{F1} and k_{F2} of I5C are 7.4×10^7 and $5.78 \times 10^7\ s^{-1}$, respectively. The ratio of the intrinsic decay parameters has therefore been assumed to be 0.727 and 0.781 for I2C and I5C, respectively, to calculate equilibrium constants. Hence, K' can be easily determined from the fluorescence quantum yield and lifetime of **1*** and **2***. The value of K' obtained for both I2C and I5C in different solvent is given in Tables 3 and 4.

TABLE 3: Relative Fluorescence Yields Q_1 and Q_2, the Equilibrium Constant, K', and Measured Lifetimes of I2C in Different Solvents

solvent	C_d[a]	Q_1 (%)	Q_2 (%)	K'	τ_{F1} (ns)	τ_{F2} (ns)
MCH	2.00	70	30	0.59	2.2	2.4
n-hexane	1.89	75	25	0.46	2.1	2.5
DEE	4.3	60	40	0.92	1.8	2.9
dioxane	7.2	49	51	1.43	1.5	3.1
THF	7.4	45	55	1.68	1.6	3.0
N,*N*-DMF	36.7	8	92	15.82	1.2	3.8
$CHCl_3$	5.14	50	50	1.37	1.9	2.4
ACN	38	6	94	21.55	1.1	4.048
EtOH	24.5	25	75	3.126	1.3	3.7
water	78.5	5	95	26.13	0.9	4.84
β-CD + water	25	19	81	5.86	1.2	4.75

TABLE 4: Relative Fluorescence Yields Q_1 and Q_2, the Equilibrium Constants K', and Measured Lifetimes of I5C in Different Solvents

solvent	C_d[a]	Q_1 (%)	Q_2 (%)	K'	τ_{F1} (ns)	τ_{F2} (ns)
MCH	2.00	75	25	0.427	1.6	2.76
n-hexane	1.89	77	23	0.382	1.56	2.89
DEE	4.3	58	42	0.93	1.5	2.9
dioxane	7.2	49	51	1.333	1.4	3.12
THF	7.4	45	55	1.567	1.34	2.87
N,*N*-DMF	36.7	9	91	12.95	1.1	4.12
$CHCl_3$	5.14	53	47	1.136	1.7	2.91
ACN	38	7	93	17.03	1.5	4.33
water	78.5				5.065	5.065
β-CD + water	25	12	88	9.39	1.9	16.3

The mechanism of Schemes 1 and 2 would suggest a double-exponential decay for **1*** emission and a buildup followed by a decay for the zwitterionic form. This mechanism is equivalent to exciplex formation, which was studied repeatedly.[29,30] Intramolecular proton transfer is, however, a mononuclear reaction and not directly related to the concentration of a reaction partner. Double-exponential decay was not resolved in any measurement reported in this paper. The relaxation of the equilibrium between **1*** and **2*** is therefore faster than the apparatus time resolution, 500 ps. Intramolecular proton transfer is generally found to be a fast process proceeding within picoseconds[31,32] or femtoseconds.[33] For the case, k_{12} and k_{21} are very much greater than k_1 and k_2, respectively.

Furthermore, a good linear correlation between the spectral shift measured between the emission maxima of **1*** and **2***, and the logarithm of excited state equilibrium constant K', is found for a large range of solvent polarities. A correlation coefficient of 0.77 and 0.69 is obtained for I2C and I5C, respectively, indicating good significance for a linear relation (Figure 9).

The Förster cycle is generally appropriate to describe the relation between changes in the pK value on excitation and the spectral shift.[34] The scheme was discussed in detail elsewhere[35,36] and can be applied to intramolecular proton transfer and this leads to the following relation between the excited-state equilibrium constant K' and the spectral shift of **2*** emission versus that arising from **1***

$$\ln K' = \ln K - \left(\frac{Nhc}{RT}\right)\Delta\nu - \left(\frac{1}{R}\right)(\Delta S^* - \Delta S) \tag{6}$$

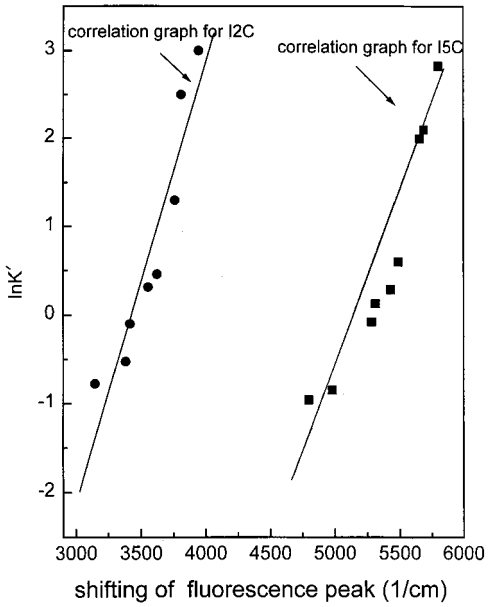

Figure 9. Correlation of ln K' and the shift $\Delta\nu$ of fluorescence maxima of **2*** vs the maximum of **1*** as a function solvent polarity for I2C and I5C.

where K is the ground state equilibrium constant, ΔS the entropy change for ground and excited state proton transfer, N Avogadro's number, h Planck's constant, c the velocity of light, R the gas constant, and T the temperature. This equation proposes a linear relationship between ln K' under the assumption that the solvent dependence of ln K and the entropy term is small. The entropy term can probably be neglected, as it is primarily determined by solvent structural relaxation which is not effective during the vertical transitions. Entropy effects are shown to play generally no dominant role in the application of the Förster cycles.[35]

Applying eq 6 and keeping ln K and the entropy term constant, a slope of 4.83×10^{-3} cm should be found. The experimentally obtained values 5×10^{-3} and 3.83×10^{-3} cm for I2C and I5C, respectively, are very near to this theoretical one. Solvent effects on ln K are therefore relatively small, and this should arise predominantly from the fact that K corresponds to nonequilibrated structures. The intercept of -19.11 is consistent with a small ground state equilibrium constant of I5C. For I2C a parallel line but with slightly larger intercept (-17.45) is obtained arising from the better proton transfer efficiency. K' values and spectral shift do not follow electrostatic solvent parameters. Specific short-range solvent interactions determine predominantly the stabilization of the zwitterionic form, and thus spectral shifts and the position of equilibrium. Nevertheless, irrespective of the specific solvent interactions, a clear-cut correlation among the excited state equilibrium constant, the spectral shift of the zwitterionic form, and its decay rate is found.

3.3. Emission at 77 K for Both I2C and I5C. In nonpolar hydroxylic glass matrix at 77 K, both the molecules are nonfluorescing. But in the presence of triethylamine (TEA), fluorescence reappeared for both the molecules. Figure 10 shows fluorescence and phosphorescence spectra of I2C and I5C in basic (TEA) MCH glass. In neutral hydrocarbon glass matrices, the proton transfer reaction ceases and hence the molecules behave like nonfluorescing agents such as normal carboxylic acid. The appearance of fluorescence and phosphorescence in the presence of amine indicates that the fluorescing species is mainly anionic in nature. But at 77 K both the molecules in ethanol glass show fluorescence and phosphorescence (Figure 11). This observation indicates that in ethanol glass matrix both the molecules take anionic forms. It is well documented that the strength on intermolecular hydrogen bonding capability increases, when we go from ethanol to ethanol glass. Due to increases in this hydrogen-bonding capability the intermolecular hydrogen bonding increases in the case of I5C with ethanol glass than that occurring at room temperature, and intermolecular hydrogen bonding occurred in I2C with ethanol glass which was hardly possible at room temperature. The intermolecular hydrogen bonding with solvent molecule increases the anionic properties of the solute, resulting in fluorescence and phosphorescence. Judging the lifetime of the phosphorescence spectra in both matrices, we come to conclusion that the emitting triplet state of anionic form of both the molecules is (π,π^*) in nature.

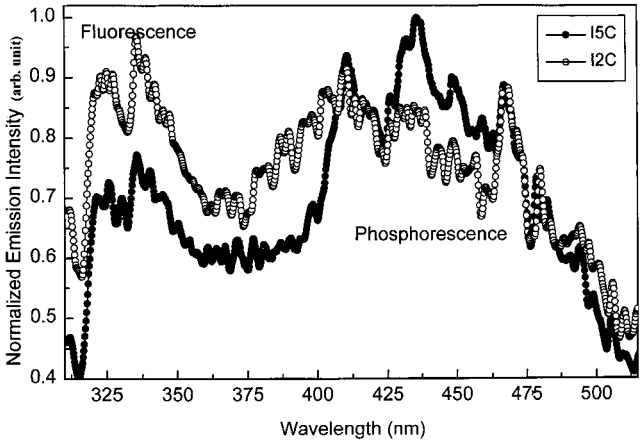

Figure 10. Fluorescence and phosphorescence emission spectra of I2C and I5C in MCH glass in the presence of triethylamine at 77 K.

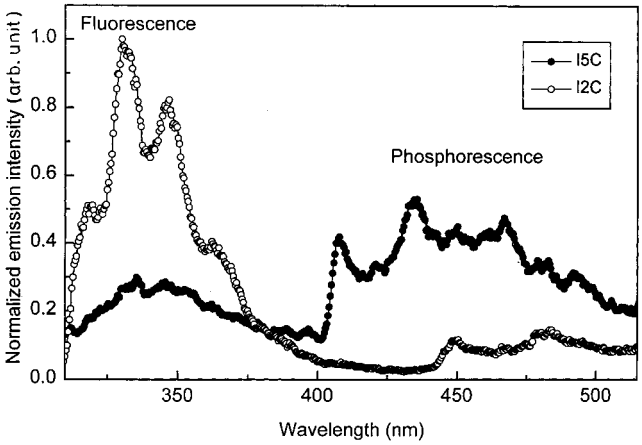

Figure 11. Fluorescence and phosphorescence of I2C and I5C in EtOH glass at 77 K.

4. Quantum Chemical Calculation

In order to have a better understanding of different excited state properties and to predict the nature and mechanism of proton transfer, the energy of electronic transitions, heat of formation, and dipole moments were calculated using the MOPAC version 5 package with AM1 Hamiltonian[37−39] for both molecules I2C and I5C in the ground and excited state. Molecular coordinates were obtained as described elsewhere.[40] A more precise geometry optimization was obtained by MOPAC's NLLSQ gradient minimization routine, and the energy of less than 0.12 cal/mol was used for optimization criterion. Excited state calculation was done with the help of CI(6×6)

which involves the interaction of microstates representing specific interaction on electrons in a set of molecular orbitals including the highest occupied (HOMO) and lowest unoccupied (LUMO) molecular orbitals, starting with a set of electronic configurations. CI calculation also provides a possible approach to calculate both the ground and excited state energies as a function of molecular geometry.

The calculated equilibrium geometries in the ground and excited state of I2C and I5C at AM1 RHF level have been depicted in Figure 12. Full geometry optimization was carried out, which showed the C−H bond lengths between 1.081 and 1.084 Å and are therefore not shown. The inter-ring bond angles generally fall within 1° of the delocalized 120°. The C−C−O and C−O−H angles in I2C are 120° and 110.1233°, respectively. In the ground state the O−H bond length of I2C is 1.003 13 Å which is a little longer than other substituted benzenes, but in the optimized excited state this O−H bond length increases and it takes the value of 1.123 103 Å. At the same time, the C−O−H increases from 110.1233° to 113.134°. Similarly, in the case of I5C, the O−H bond length in the optimized ground state geometry is 0.996 16 Å, but in the optimized excited state geometry it increases to 1.13423 Å. This structural change indicates the possibility of proton transfer in the excited states of I2C and I5C molecules. The total electronic energy, heat of formation (enthalpy), and dipole moments in the ground and excited state of the optimized structure are shown in Table 5. Table 5 shows that for both molecules there are large changes in dipole moments when one goes from ground state to excited state. This large change in dipole moment is only accounted for by charge redistribution in excited state and that is only possible in the case of intramolecular proton transfer from the acid moiety to the base moiety of I2C and I5C molecules.

Now the potential energy curves in the excited states of both molecules are distorted along the O−H coordinate relative to the ground state. In the ground state the potential energy has a single minimum whereas in the excited state they have two minima. This double minima in the excited state potential energy may be due to slow $ESI_{ra}PT$ rate.

The dependence of ground state singlet energy (S_0) in I2C and I5C on O−H bond distance has a prominent effect showing activation barrier; i.e., on increasing the O−H bond distance (Figure 13) S_0 energy increases. These findings confirm that in the ground state proton transfer is not possible. On the other hand, from excited state CI(6×6) calculations we observe the energy dependence of the first two excited singlet states S_1 and S_2 with O−H bond distance. Figure 13 shows the variation of S_0, S_1, and S_2 state energy with O−H distance for I2C and I5C, respectively. The first excited state singlet energy shows a minimum for a particular O−H bond distance and it is 1.133 103 Å for I2C and 1.192 341 Å for I5C. But the second excited singlet state (S_2) energy increases with the increase in O−H bond distance almost linearly. This nature of first excited state singlet energy combined with the fact of having proton transfer tendency in the first excited singlet state of both molecules shows dual fluorescence characteristics. The difference between S_1 and S_0 energy fairly matches with the experimentally obtained fluorescence peak. For I2C it exactly coincides with two fluorescence peaks but for I5C there is little difference, but within tolerable limits.

The dipole moment and heat of formation show a strong variation with O−H bond distance when other coordinates of ground state optimized geometry are kept unaltered. On increasing the O−H bond distance, both dipole moment and heat of formation energy continuously increase (Figure 14). This change in dipole moment confirms the proton transfer affinity of both the molecules, and the increase of heat of formation indicates the necessity of external energy to transfer a proton from the O−H group to the basic moiety of the molecules. So proton transfer is possible only by exciting the molecule, which we call excited state intramolecular proton transfer.

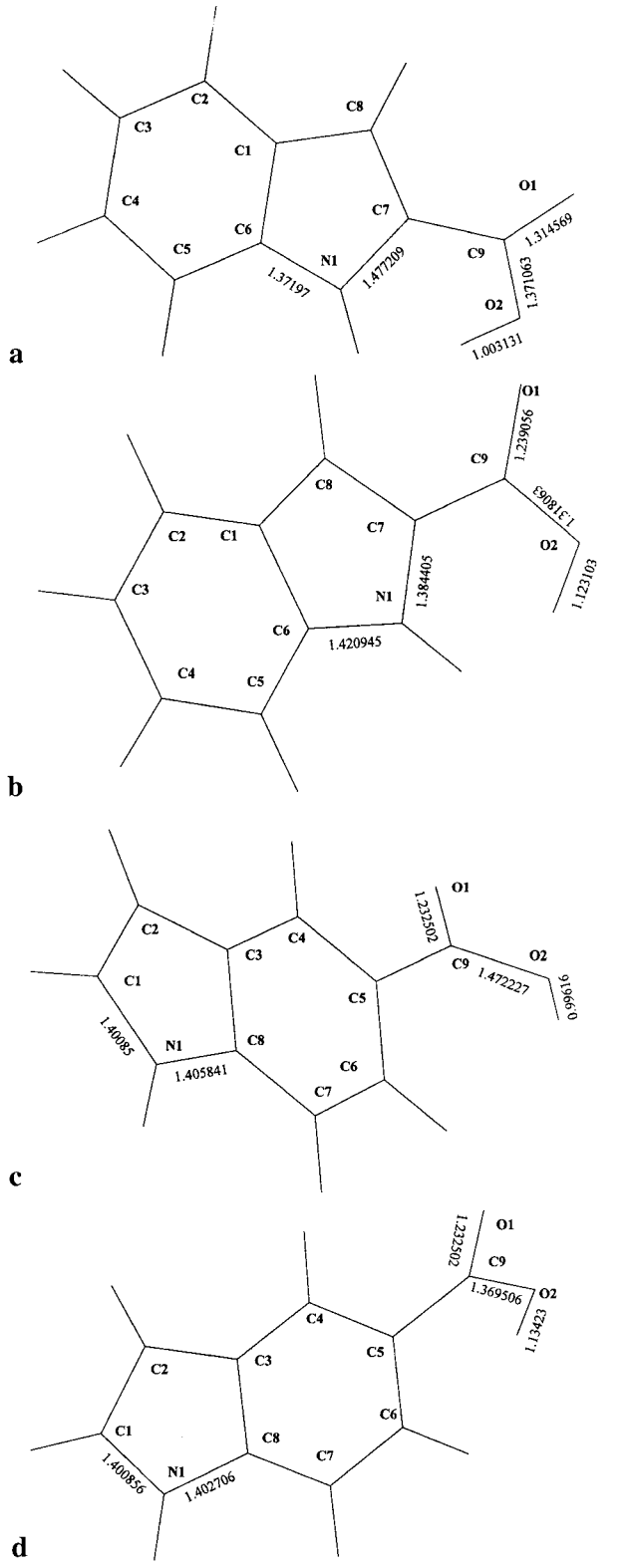

Figure 12. (a) Optimized geometry of I2C in the ground state. (b) Optimized geometry of I2C in the excited state. (c) Optimized geometry of I5C in the ground state. (d) Optimized geometry of I2C in the excited state.

TABLE 5: Final Heats of Formation, Dipole Moments, and Total Electronic Energy of I2C and I5C in Ground and Excited State[a]

molecule	ΔH_f (kcal/mol)	dipole moment (debye)	electronic energy (eV)
I2C	−39.323 48 (Gr)	4.533 13 (Gr)	−2096.002 81 (Gr)
	71.402 44 (Ex)	6.737 12 (Ex)	−2091.201 37 (Ex)
I5C	−30.500 35 (Gr)	7.062 (Gr)	−2095.620 21 (Gr)
	70.501 41 (Ex)	9.185 (Ex)	−2091.240 23 (Ex)

[a] Gr, ground state; Ex, excited state.

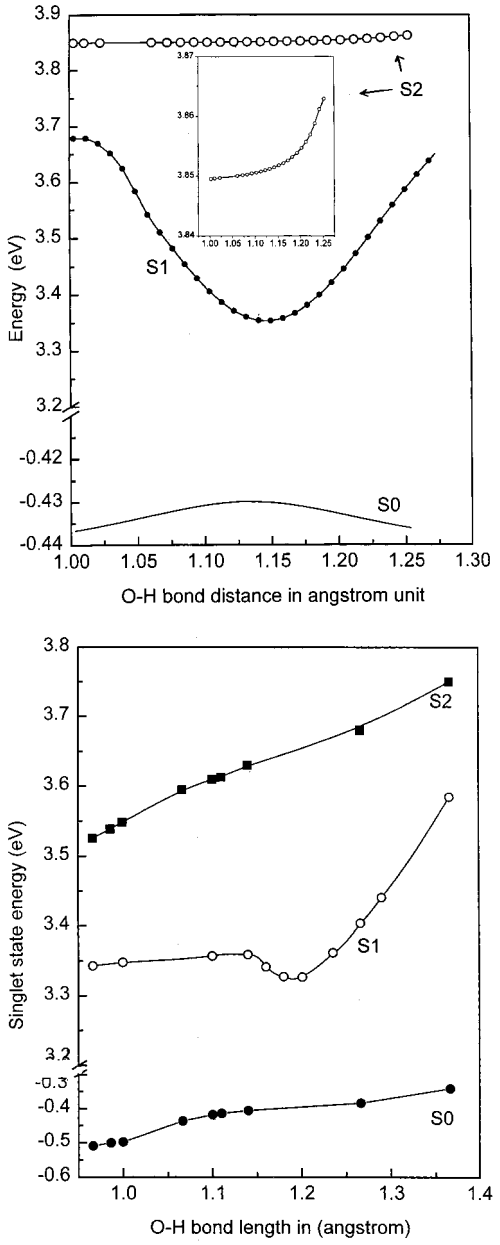

Figure 13. (a, top) Variation of S_0, S_1, and S_2 energy with O−H bond distance of I2C and inset shows the variation of S_2 energy in close view. (b, bottom) Variation of S_0, S_1, and S_2 energy with O−H bond distance of I5C.

Now in the light of above quantum chemical calculations, the expected mechanism of dual fluorescence of I2C and I5C may be through energetically advantageous intramolecular relaxation involving transfer of a proton from the acid group of the molecules to the basic group. On excitation, the molecules achieve delocalized excited state and then relax to proton transfer configuration, taking part in lower energy fluorescence.

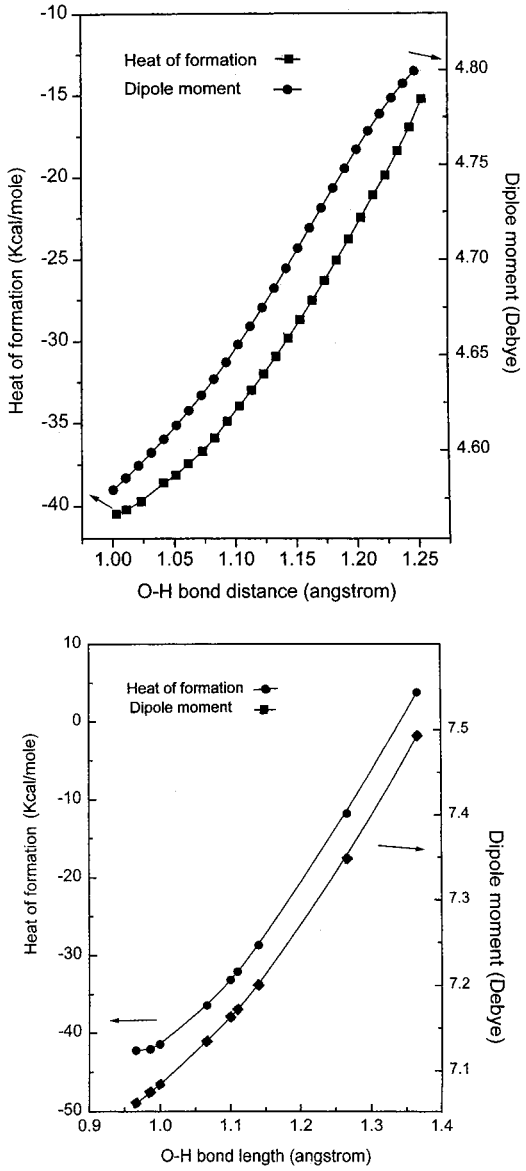

Figure 14. (a, top) Variation of heat of formation and diapole moment as a function of O−H bond distance keeping the ground state geometry fixed for I2C. (b, bottom) Variation of heat of formation and dipole moment as a funcition of O−H bond distance keeping the ground state geometry fixed for I5C.

5. Conclusion

1. I2C exhibits broad structureless fluorescence in all protic, aprotic, polar, and nonpolar solvents independent of excitation energy, which are composed of two hidden bands. One band is attributed to the neutral indole form, the other at lower energy to the zwitterionic proton transferred form.

2. I5C shows dual fluorescence in hydrocarbon medium and broad structureless red-shifted fluorescence spectra in non-hydroxylic polar medium. The fluorescence spectra of polar medium are composed of two bands one higher energy band and other lower energy band. These two bands in hydrocarbon and aprotic polar medium are attributed to be from neutral and proton transferred zwitterionic form.

3. The spectrum of the doubly ionized form of I5C is shifted strongly toward red than the spectrum of the same form of I2C, indicating considerably larger solvent stabilization of the excited state due to the large separating distance of the positive and negative charges in I5C than I2C.

4. For I2C, excited state proton transfer occurred both in hydroxylic solvent and within the β-CD cavity, but for I5C that happens only in the β-CD cavity.

5. For both molecules, solvent polarity dependent shift of fluorescence spectrum indicates considerably large solvent stabilization of the excited state than that of the ground state. Independent of specific short-range interactions, a good correlation between the spectral shift of the zwitterionic form and excited state equilibrium constant K' was found, according to the well-established Förster cycle.

6. The anionic form of both the molecules shows phosphorescence. At 77 K in alcoholic glass, intermolecular hydrogen bonding occurred betweent I2C and the solvent, stopping the intramolecular proton transfer reaction.

7. Finally, quantum chemical calculations confirm that the excited state proton transfer is energetically favorable in the case of I2C and I5C whereas proton transfer in the ground state is not possible.

Acknowledgment. The authors express their deep sense of gratitude to Prof. S. Basak, SINP, Calcutta, for kindly allowing them to use the fluorescence lifetime measuring instrument. The authors also thank Prof. P. C. Mishra, Physics Department, Banaras Hindu University, India, for kindly making available the MOPAC (version 5) package to them.

References and Notes

(1) Cha, Y.; Murray, C. J.; Klinman, Z. J. P. *Science* **1989**, *243*, 1325.
(2) Desiraju, R. *Acc. Chem. Res.* **1991**, *24*, 290.
(3) Hilbert, F. *Adv. Phys. Org. Chem.* **1986**, *22*, 113.
(4) Müller, A.; Ratajcak, H.; Junge, W.; Diemann, E. *Electron and Proton Transfer in Chemistry and Biology*; Studies in Physical and Theoretical Chemistry; Elsevier: Amsterdam, 1992; Vol. 78.
(5) Weller, A. *Z. Electrochem.* **1956**, *60*, 1144.
(6) van Benthem, M. H.; Gillispie, G. D. *J. Phys. Chem.* **1984**, *88*, 2954.
(7) Mordzinski, A.; Grabowska, A.; Teuchner, K. *Chem. Phys. Lett.* **1984**, *11*, 383.
(8) Ghiggino, K. P.; Scully, A. D.; Leaver, H. I. *J. Phys. Chem.* **1986**, *90*, 5089.
(9) Nishiya, T.; Yamauchi. S.; Hirota, N.; Baba, M.; Hanazaki, I. *J Phys. Chem.* **1986**, *90*, 5730.
(10) Becker, R. S.; Lenoble, C.; Zein, A. *J. Phys. Chem.* **1987**, *91*, 3509.
(11) Kosower, E. M.; Huppert, D. *Annu. Rev. Phys. Chem.* **1986**, *37*, 127.
(12) Dick, B. *Ber. Bunsen-Ges. Phys. Chem.* **1987**, *91*, 1205.
(13) Chou, P.; Morrow, D. Mc.; Artsma, T. J.; Kasha, M. J. *Phys. Chem.* **1984**, *88*, 4596.
(14) Harrah, L. A.; Renschler, C. L. *Nucl. Instrum. Methods Phys. Revs. Sect. A* **1985**, *A235*, 41.
(15) Catalan, J.; Fabero, F.; Guijarro, Ms.; Claramrent, R. M.; Santa Maria, M. D.; Focen Foces, M. C.; Cano, F. H.; Elguero, J.; Sastree, R. *J. Am. Chem. Soc.* **1990**, *112*, 747; correction *J. Am. Chem. Soc.* **1991**, *113*, 4046.
(16) Smith, T. P.; Zalika, K. A.; Thakur, K.; Walker, G. C.; Tomianaga, K.; Barbara, P. F. *J. Photochem. Photobiol. A Chem.* **1992**, *65*, 165.
(17) Bangal, P. R.; Chakravorti, S. *Indian J. Phys.* **1998**, *72B*, 655.
(18) Bortulos, P.; Monti, S. *J. Phys. Chem.* **1987**, *91*, 5046.
(19) Yorozu, T.; Hoshino. M.; Imamura, M. *J. Phys. Chem.* **1982**, *86*, 4426.
(20) Chattopadhyay, N. *J. Photochem. Photobiol. A* **1991**, *58*, 31.
(21) Hamal, S. *Bull. Chem. Soc. Jpn.* **1996**, *69*, 543.
(22) Rao, C. N. R. *Chemical Applications of Infrared Spectroscopy*; Academic Press: New York, 1963.
(23) Shanbhag, P. V.; Shashidhar, A. M.; Rao, S. K. *Indian J. Phys.* **1984**, *58B*, 174.
(24) **)** Badger, R. M.; Bauer, S. H. *J. Chem. Phys.* **1937**, *5*, 839.
(25) **)** Badger, R. M. *J. Chem. Phys.***1940**, *8*, 288.
(26) Zadorozhnyi, B. A.; Ishchenko, I. K. *Opt. Spectrosc.* **1965**, *19*, 306.
(27) Bangal, P. R.; Chakravorti, S. *Opt. Mater.*, communicated submitted for publication.
(28) Cramer, L. E.; Spears, K. G. *J. Am. Chem. Soc.* **1978**, *100*, 21.
(29) Connor, D. V. O.; Phillips, D. *Time-correlated Single Photon Counting* Academic Press: New York, 1984.
(30) Connor, D. V. O.; Ware, W. R. *J. Am. Chem. Soc.* **1976**, *98*, 4708.
(31) Smith, K. K.; Kaufmann, K. J. *J. Phys. Chem.* **1978**, *100*, 2286.
(32) Barbara, P. F.; Rentzepis, P. M.; Brus, L. E. *J. Am. Chem. Soc.* **1980**, *102*, 2786.
(33) Mitra, S.; Tamai, N. *Chem. Phys. Lett.* **1998**, *282*, 391.
(34) Förster, Th. *Z Electrochem.* **1950**, *54*, 197.
(35) Grabowski , Z. R.; Grabowska, Z. *Phys. Chem.* **1976**, *101*, 197.
(36) Grabowski, Z. R.; Rubaszewska, W. J. *Chem. Soc., Faraday Trans 1* **1977**, *73*, 11.
(37) Stewart, J. J. MOPAC Program 455, Quantum Chemistry Program Exchange, University of Indiana, Bloomington, IN.
(38) Dewar, M. S. J.; Thiel, W. *J. Am. Chem. Soc.* **1977**, *99*, 4899.
(39) Dewar, M. S.; Zoebisch, E. G.; Healy, E. F.; Stewart, J. J. *J. Am. Chem. Soc.* **1985**, *107*, 3902.
(40) Bangal, P. R.; Chakravorti, S.; Mostafa, G. *J. Photochem. Photobiol.* **1998**, *113*, 35.